



Olive Mill Solid Waste Characterization and Recycling opportunities : A review

H. Ouazzane^{1,*}, F.Laajine¹, M. El Yamani², J. El Hilaly^{1,3}, Y. Rharrabti²,
M-Y. Amarouch^{1,3}, D. Mazouzi^{1,3,*}

¹Materials, Natural Substances, Environment and Modeling Laboratory, Multidisciplinary Faculty of Taza, University of Sidi Mohamed Ben Abdellah-Fes, Morocco.

²Laboratory of Natural Resources and Environment, Multidisciplinary Faculty of Taza, University of Sidi Mohamed Ben Abdellah-Fes, Morocco.

³Biology, Environment & Health Team, Department of Biology; Faculty of Sciences and Techniques Errachidia (FSTE), University of Moulay Ismail Meknes, Morocco.

Received, 22 Jan 2017

Revised, 27 Mar 2017

Accepted 31 Mar 2017

Keywords

- ✓ OMSW;
- ✓ Activated Carbon;
- ✓ Combustion;
- ✓ Pyrolysis

D Mazouzi

driss.mazouzi@usmba.ac.ma

Phone: +212535211976

H. Ouazzane

houssam.ouazzane@usmba.ac.ma

Phone: +212658902954

Abstract

In the past decay, the olive by-products were used for various applications. Indeed, many studies have been focused on the exploitation of olive mill solid waste (OMSW) derived from discontinuous or continuous processing of olive fruits. In this review, thermochemical and physical valorisation pathways of solid olive mill residues are described. OMSW characterization in term of chemical properties, as well as its thermochemical decomposition behavior, play key roles for the optimization of the final product, the understanding of the raw material properties, the prediction of OMSW behavior under known conditions, and conceiving a better process for treatment. In this context, the aim of the study was to revise the current literature characterizing and valorizing olive mill solid wastes.

1. Introduction

The olive oil industry is very important in Mediterranean countries, both in terms of wealth and tradition. The olive oil market has hugely expanded over the two last decades, its worldwide production has increased from 1.4 in 1990/1991 to 3.2 million tons in 2015/2016 [1]. This production keep growing due to the nutritional benefits and economic interest of this substance [2].

The olive oil industry generates huge quantities of high polluting by-products, namely wastewater and solid waste. The former consists of the combination of vegetation olive water, and the one added to facilitate the oil separation during the extraction process, while the latter is composed of seeds and pulp residual fractions. Olive oil extraction can generate up to 30-40 % of solid waste, depending on its moisture and the olive fractions content in the fruit, as well as, the extraction process [3]. More specifically, the world municipal solid waste production is approximately 1300 million tons per year [4] and it is estimated that, in 2025, the production will rise to 2200 million tons per year with approximately 46% organic contents. A small portion of these wastes can be used as raw materials in different industries as they contain valuable natural resources.

On the other hand, there are studies indicating that the Olive Mill Solid Waste (OMSW) may also be regarded as an economic resource. They has been directly exploited on various applications such as direct combustion [5], soil amendment [2], and livestock feeding [6]. However, the inefficiency and the environmental risks have limited these use pathways. Indeed, OMSW represents high moisture, and moderate oxygen contents [7] that limit the heating value of OMSW and increases technical constraints and environmental risks (deposition, corrosion, and high polluting emissions [8, 9]). Furthermore, the OMSW chlorine content exceeded the tolerable content value (> 0.7 % in the pulp fraction). At this level, its use in the soil amendments may lead

to phytotoxicity and soil acidification via HCl formation. Regarding the OMSW use in combustion may induce the formation of high toxic chemicals such as dioxins and furans [9]. Furthermore, the OMSW may be as an inexpensive source of inorganic and organic compounds to be recovered because of their potential economic interest or their ability to be transformed into products for use in agriculture, biotechnology, and the pharmaceuticals industry as well as in the food industry[10].

For all these reasons, OMSW characterization and valorization become one of the important research field aiming to protect the environment via the promotion of waste management and renewable energy research. The selection of the conversion technology depends on the desirable specific application. Therefore, the investigation of the physicochemical characteristics of the processed feedstock and the understanding of the phenomena taking place during the pretreatment and processing of solid olive wastes, as well as of the parameters affecting the final product, are necessary and fundamental importance and factor for optimizing the utilization processes, predicting and evaluating the thermal performance and use of solid olive wastes for this various applications.

Thus, this study aims to highlight a summary of updated information on research works that propose different characterization and valorization methods based on scientific studies, with particular attention was devoted to thermochemical treatment and physical processes laying special emphasis on Olive Mill Solid Waste.

2. Olive oil extraction processes

To extract olive oil, three methods are commonly used such as the traditional press method, the three-phase and the two-phase decanter centrifuge methods. For the traditional method, the ground paste is placed between pressing mats and is subject to pressure, to expel the oil mix (mixture of oil and water). The mixture is then poured into a vat or holding tank. This is allowed to rest so that gravity and different densities come into play, separating the oil from the water. While, the three-phase process is based on a three phase decanter such as 1 litre of water is added per kilo of paste; it is then added to a horizontal centrifugal machine, where the solid is separated from the oil must. The must is then passed on to a vertical centrifugal machine, where the oil is separated from the vegetable water. However, the process based on a two-phase decanter same of process as above, but instead of adding water for the horizontal centrifugation, the vegetable water is recycled (figure 1).

The main differences between the extracted raw materials are that the two-phase olive mills generate two types of steams: olive oil steam, and a mixed steam which combines solid and liquid wastes. While, the three-phase and pressing processes generate three types of steams: olive oil, wastewater, and solid waste [4]. On the other hand, two-phase pomace has moisture approximately 50-70% and contains a certain amount of sugars as a result of the presence of vegetation water, while traditional pomace has a moisture content of between 25-30% in the pressing system, and 45-60% in three-phase centrifugal systems

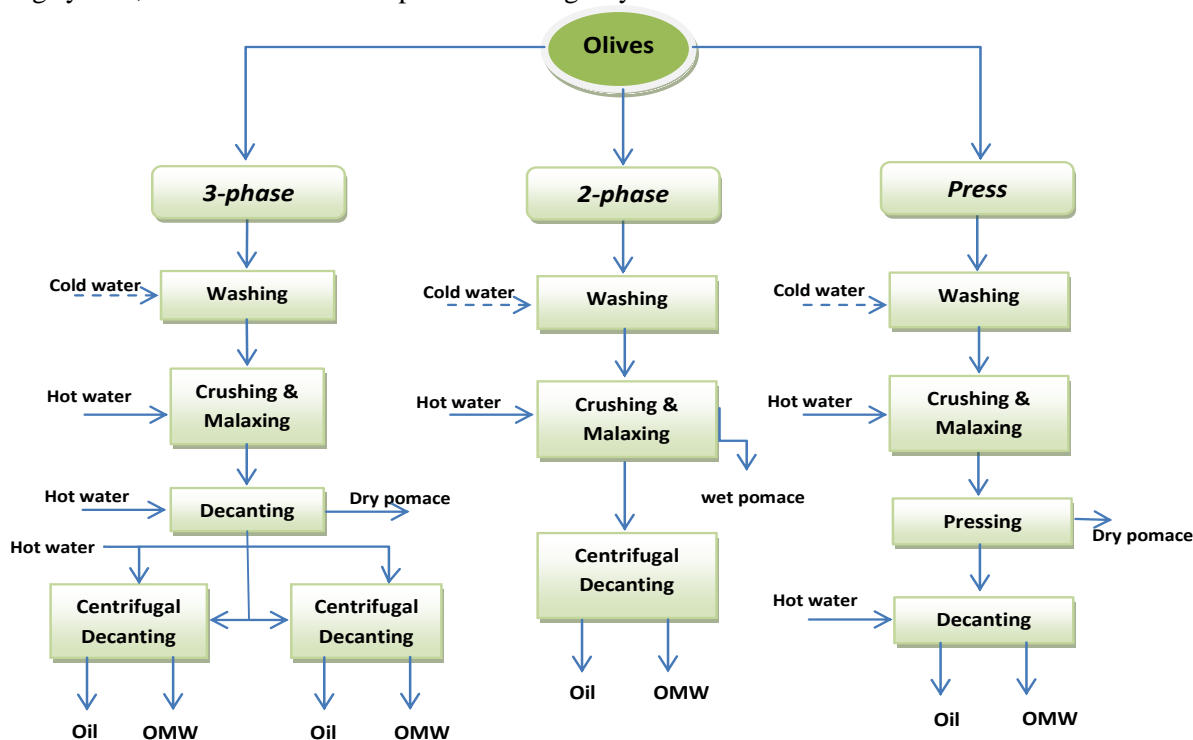


Figure 1: Key information of the olive oil extraction technologies. (Figure adapted from: [2,11])

3. Chemical characterization of olive oil solid waste

The chemical characterization of specific biomass is crucial to determine the environmental hazards during its life cycle as well as to choose the optimal options for treatments or valorization [12]. The characteristics of OMSW (also known as, olive pomace, olive husk, alperujo, or olive solid residue) may depend on several parameters, namely, parent olive species, culture conditions, extraction process, and storage conditions [11].

To characterize biomass wastes, many analysis techniques have been used [12]. The current review aims to present relevant information concerning Proximate Analysis, Ultimate or Elemental Analysis, Ash Analysis, Structural Composition, Gross Calorific Value, and Surface area and Porosity Characterization.

3.1 Proximate analysis

The proximate analysis aims to characterize the biomass via the evaluation of its content on moisture (M), the fixed carbon (FC) fraction, the volatile matter (VM) fraction, and the ash yield (A) [12].

3.1.1 Moisture content

The moisture content of different studied OMSW samples varied considerably, depending on several parameters, in particular the oil extraction process. Indeed, two-phase, three phase and pressing olive mill solid wastes have a different chemical composition, particularly for the moisture content (55-75%, 40-45%, and 20-25%, respectively, for the two-phase, three phase, and pressing processes), due to the difference on necessary water amount between the three processes [11, 13]. The two-phase olive mill solid waste (TPOMSW) represents the higher moisture content compared to the wastes coming from the three phase and pressing processes [7]. Indeed, TPOMSW moisture content value has reached 70% [7]. This composition represents real constraints for its storage, transportation, and treatment [7]. To allow further comparison between the properties of different OMSW samples, a drying pre-treatment is highly recommended [7, 14-16]. Hence, the following OMSW characteristics are determined in dry basis.

3.1.2 Volatile Matter (VM)

The volatile matter (VM) represents around three quarters of OMSW total weight (*dry basis*). Indeed, the VM yield varies between 65% [17] and 82% [18] in weight basis (*wt%*). On the other hand, It has been shown that VM content varies slightly throughout the different OMSW components [9]. The pit, the pulp and the residual olive cake (ROC) fractions consisted of 80.9%, 79.1% and 77.8% of (VM) (*wt%*), respectively [9].

3.1.3 Fixed carbon (FC)

Previous studies have shown significant difference in the fixed carbon (FC) yield: 12.31% [7] and 21.1% [15]. The pulp fraction shows the poorest fraction on (FC) with 15.3% , while the pit fraction represents 18.5% of total weight [9].

3.2 Ultimate composition

The Ultimate analysis allows to determine the percentage of Carbon (C), Hydrogen (H), Nitrogen (N) and Sulphur (S) in the total weight of OMSW [12]. Samples are burned with an excess of oxygen, then, the mass of the combustion products (NO₂, CO₂, SO₂ and H₂O) are used to calculate the percentages of the contained elements (N, C, S and H, respectively). The (O) content is deducted by subtracting the percentages sum of N, C, S and H elements to 100 % [7].

3.2.1 Carbon content (C)

The carbon (C) represents the most abundant element in OMSW. Indeed, the carbon content has been described to vary between 46.8% [19] and 57.8% [7]. Moreover, the distribution of carbon element is quasi-equitable throughout olive pit (52.27%), olive pulp (55.20%) and residual olive cake (54.89%) [9].

3.2.2. Oxygen content (O)

The oxygen (O) is the second most available element present in the OMSW. In this sense, several studies have shown the variation of (O) content between 34% [7, 9] and 45% [15, 17]. These differences may be related to the olive chemical composition, the extraction process, or the storage conditions.

3.2.3. Hydrogen content (H)

The hydrogen (H) content is an important indicator for the energy density of OMSW, especially for the efficiency of gasification processes [5]. According to literature, its value did not exceed 10% of the total weight of OMSW (from 5.8% [15] to 9.2% [20]).

3.2.4. Nitrogen content (N)

The (N) content is an important indicator of the toxic emissions related to the biomass combustion. Indeed, due to its contribution to the production of nitrogen oxides, the (N) content should not exceed 0.6% of the total combustible weight. In fact the olive pit is the suitable OMSW fraction for direct combustion [9]. The nitrogen (N) content of OMSW varies between 0.6% [7, 20] and 2.7% [21]. The olive pit shows the poorest fraction in (N) (around 0.1 %) [9], while it reached 2% of the total weight in the other fractions (pulp and residual cake) [9].

3.2.5 Sulphur content (S)

Sulphur (S) is the lowest element contained in OMSW. Its percentage does not exceed 0.16% of total weight [21].

3.3 Structural composition

The OMSW belongs to the lignocellulosic biomass. Indeed, its main components are cellulose, hemicellulose and lignin [12].

3.3.1. Hemicellulose

Also known as polyose, the hemicellulose is a branched polymer with the following chemical formula: $(C_5H_8O_4)_m$; where m represents the polymerization degree [22]. The main components of hemicelluloses are xylose, glucose, mannose, galactose, arabinose and glucuronic acid [22]; and the atomic ratios of O/C and H/C are around 0.80 and 1.60, respectively [22]. Finally, the hemicellulose shows an exothermic degradation occurring between 220 and 315 °C [22]. In OMSW, the hemicellulose content varies from 14.4% [18] to 36.58% [7] of the total weight.

3.3.2. Cellulose

The cellulose is a linear glucosan polymer, with the chemical formula $(C_6H_{10}O_5)_m$. Its atomic ratios of O/C and H/C are around 0.83 and 1.67, respectively [22]. The thermal degradation of cellulose occurs at the temperature range of 315-400 °C. Furthermore, the thermal decomposition of cellulose shows an endothermic behavior, as long as, the char formation is not significant [22]. According to literature, the OMSW cellulose content differs considerably between the two phase and three phase processes (36.6% and 24.1% of the total weight of OMSW, respectively) [20]. Moreover, the olive pit shows the richest part of OMSW in cellulose in comparison to pulp and residual olive cake (ROC) [9].

3.3.3. Lignin

The lignin is a complex phenolic polymer with a three-dimensional structure. Its atomic O/C and H/C ratios vary between 0.47-0.36 and 1.19-1.53, respectively [22]. The thermal degradation of lignin is an exothermic phenomenon, that, starts at around 160°C and continues up to 900°C [22]. According to literature, the lignin fraction, in OMSW, varies from 20.3% [20] to 43.2% [7].

3.4. Ash analysis

Using X-ray fluorescence (XRF), the ash analysis of OMSW aims to characterize the composition of residual ash after char oxidation [7]. The main elements characterized are Si, Al, Fe, Ca, S, Mg, K, Ti, Na, P, Mn, and Cl [12]. The most abundant elements in OMSW ash are potassium (K) (16020-28434 mg/kg) followed by calcium (Ca) (1693-3219 mg/kg) [20, 23]. The sodium (Na), magnesium (Mg) and iron (Fe) are also present in considerable quantities (104-214 mg/kg, 511-808 mg/kg and 87.4-302 mg/kg, respectively) [20, 23]. A prominent way to exploit the combustion residues was proposed by De la Casa and Castro. Indeed, its low thermal conductivity (0.13-0.16 W/m K), its minimum bulk density (1790-1810 kg/m³) and its bending strength (10-12 Nmm⁻²) make it a potential candidate for masonry bricks use [24].

3.5. Gross Calorific Value (GCV)

According to diverse investigations in the energy content of OMSW, many formulas of gross calorific value have been proposed, as a function of W_C , W_H , H_O , W_N and W_S (weight content(%) of Carbone, Hydrogen, Oxygen, Nitrogen and sulfur, respectively):

Dulong equation:

$$GCV = 8140 * W_C + 34400 * (W_H - W_O/8) - 0.12 * W_N + 2220 * W_S \text{ (Kcal/Kg) [7]}$$

Combined with experimental data, a modified Dulong formula has been proposed by[21]:

$$GCV = 32.79 * W_C + 150.40 * W_H - 3.83 * W_O - 2.42 * W_N + 9.26 * W_S$$

Moreover, The low (N) and (S) factors and contents in OMSW in the previous equation might be interpreted as a low contribution of the both elements in the total GCV[21]. Hence, the modified Dulong formula could be simplified as follows:

$$GCV = 32.79 * W_C + 150.40 * W_H - 3.83 * W_O$$

Milne equation:

$$GCV = 0.314 * W_C + 1.322 * W_H - 0.12 * W_O - 0.12 * N + 0.0686 * W_S - 0.0153 * W_{Ash} \text{ (MJ/Kg)[7].}$$

The GCVs formulation,as well as, the obtained experimental values varies from an author to another. Indeed, using the bomb calorimetrictools, the GCV raw value of OMSWwas around 18.2 MJ/Kg [15]. However, its reach more important values from two phase and three phase processes (22.3 MJ/Kg and 21.7 MJ/Kg, respectively)[20].Moreover, the pulp fraction represented the higher GCV value(23.39MJ/Kg), followed by olive pit (22.49MJ/Kg)and residual olive cake (20.61MJ/Kg)[9].

3.6. Surface area and porosity

Surface area and porosity are capital properties which determine oxidation, adsorption/desorption and catalytic behavior of OMSW [7]. The table.1 shows the influence of several treatments on surface proprieties of OMSW and olives stones (OS) precursors.According to literature, the surface area of raw OMSW and olive stones varied between 0.16m²/g and1.24m²/g[7, 16, 25,26]. The internal surface of raw OMSW represented around 27% of whole surface area[7]. It has been considerably enhanced to reach 500, 1800 and 1500m²/g using carbonization, chemical treatment and physical treatment, respectively table 1. Furthermore, the porosity of raw OMSW and olive stones (around 8.94 x 10⁻⁴ cm³/g) was dominated by macro-pores around 83%, while mesopores represented less than 8%[16] The chemical activation allowed more development of micropores (more than 80%) of total pores volume which reached 0.859cm³/g[27] as shown in table.1. In turn, the porosity of physical activated OMSW and OS has been considerably enhanced in term of micropores development except for high carbonization temperatures, where samples showed high macropores development (up to 53% of total pores volume)[28, 29].

Table 1: Main surface area and porosity characteristics of olive oil solid waste and olives stones.

Table 1a: Without activation

Raw material	Chemical agent	Pyolysis	Specific area (m ² /g)	Total pores volume (cm ³ /g)	V _{micro}	V _{meso}	V _{macro}	Reference
Without activation								
OMSW	-	-	1.24	-	-	-	-	[25]
OMSW	-	-	0.74	8.94x10 ⁻⁴	-	-	-	[7]
OS	-	-	0.60	-	-	0.03	0.16	[16]
OS	-	-	0.16	1.84x10 ⁻³	-	-	-	[26]

Table 1b: Carbonisation, chemical and physical activation

Raw material	Chemical agent	Pyolysis	Specific area (m ² /g)	Total pores volume (cm ³ /g)	V _{micro}	V _{meso}	V _{macro}	Reference
Carbonisation								
OS	-	800°C for 1h	500	-	-	-	-	[30]
OMSW	-	450°C for 2h	150	-	-	-	-	[31]
Chemical activation								
OMSW	H ₃ PO ₄ at 85°C for 4h	450°C for 2h	400	-	-	-	-	[31]
OMSW	ZnCl ₂ at room temp for 24h	450°C for 2h	1480	-	-	-	-	[31]
OS	ZnCl ₂ at 800°C	700°C for 1h	735	-	-	-	-	[30]
OMSW	KOH at 600°C for 1h	400°C for 1h	673	0.346	0.28	0,06	-	[32]
OMSW	KOH at 800°C for 3h	800°C for 1h	1839	0.859	0.72	0.14	-	[27]
OMSW	H ₃ PO ₄ at 85°C for 3h	500°C	958	0.440	0.38	0.06	-	[33]
OS	Oxidized by HNO ₃ at 60°C for 24h	500°C	738	0.370	0.30	0.07	-	[33]
Physical activation								
OS	Steam at 750°C	600°C for 1h	807	0.710	0.30	0.41	-	[34]
OMSW	Steam at 800°C for 2h	800°C for 10min	1030	0.665	0.36	0.11	0.20	[28]
OS	Steam at 850°C for 30min	600°C for 1h	813	0.555	0.46	0.10	-	[35]
OMSW	Steam at 800°C for 1h30min	850°C for 1h30min	914	1.560	0.36	0.37	0.83	[29]
OS	CO ₂ at 900°C for 8h	700°C for 2h	1591	0.750	0.62	0.13	-	[36]
OMSW	Steam at 850°C for 45min	500°C	803	0.472	0.30	0.17	-	[37]

4. Thermochemical decomposition (thermolysis) of OMSW

Several thermochemical conversion processes (Drying, torrefaction, pyrolysis, combustion, gasification) of OMSW have been studied using thermogravimetric analysis (TGA) [20]. The experimental data, (TG) and (DTG) curves figure.2 and figure.3, allowed to understand and describe the process mechanism into different

stages which aim to simplify the whole conversion process into a scheme of reactions[38]. The understanding of the material behavior at each stage, as well as, the interactions between the different stages are the keys of a better analysis of thermal decomposition kinetics [39].

4.1. Thermal decomposition mechanism

4.1.1 Pyrolysis mechanism of OMSW

TG and DTG curves from previous studies, (Figure.2), four mass loss regions from DTG curves of which each region is distinguished by an associated peak temperature [7]. The first region corresponds to the moisture evaporation ($T < 180\text{ }^{\circ}\text{C}$) [39], ($100 < T < 200\text{ }^{\circ}\text{C}$) [7]). The second and third regions corresponds to the cellulose and hemicellulose decomposition, where volatile compounds were formed ($180 < T < 500\text{ }^{\circ}\text{C}$) [39], ($250 < T < 400\text{ }^{\circ}\text{C}$) [7]). The last region corresponds to a high temperature decomposition ($T > 500\text{ }^{\circ}\text{C}$) [39], ($400 < T < 600\text{ }^{\circ}\text{C}$) [7] where the most contribution comes from lignin and extractives decomposition [7]. The delay in stages between different investigations is due generally to the difference in experimental conditions (*i.e.* heating rate, particle size, crucibles, etc) [40].

The first stage, which corresponds to the water evaporation, is often ignored during pyrolysis investigations of OMSW [7, 39,41]. Indeed, the large variation of OMSW moisture content throughout the studied samples may affect significantly this first step[13]. Furthermore, The drying phenomena is often considered as a simple diffusion mechanism[41], contrary to the complexity of volatilization and high decomposition mechanisms, where several heterogeneous reactions occur[38].

In fact, the pyrolysis process of OMSW could be described by two main consecutive steps, (i) the primary pyrolysis regrouping the hemicellulose and the cellulose decomposition regions, and (ii) the secondary pyrolysis that corresponds to the high decomposition region [42].

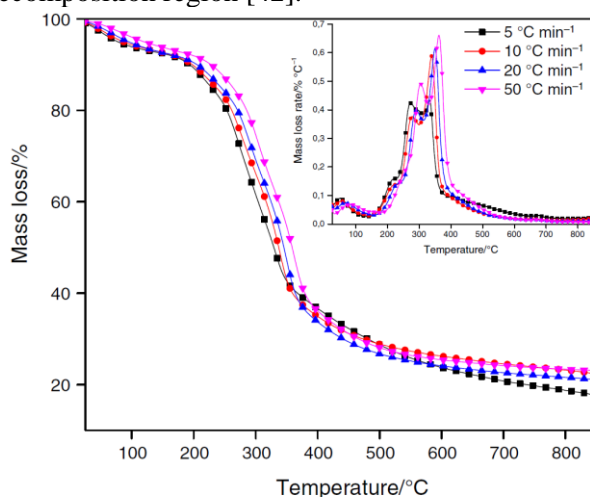


Figure.2: TG and DTG curves of OMSW (copyright permission[43])

4.1.2 Combustion mechanism

The figure.3, which illustrates the DTG curves of OMSW combustion shows three main mass loss regions[20]. The first mass loss region represents the moisture evaporation (drying) of the decomposed OMSW. The second mass loss region corresponds to the OMSW oxidative degradation, and occurs between 249-353 $^{\circ}\text{C}$ [44]. The main contributors to this stage mass loss are hemicellulose and cellulose, whereas the lignin fraction contributes slightly in this phase[45]. Finally, the last mass loss region corresponds to the char oxidation stage, and occurs between 414-627 $^{\circ}\text{C}$ [44]. During this stage, the respective chars, produced during oxidative degradation, react with oxygen [46]. The temperature range of each pre-cited stage varies considerably in function of the experimental conditions [45, 47]. Indeed, the temperature range of the first and second stages delay, respectively, from 180-290 $^{\circ}\text{C}$ and 290-470 $^{\circ}\text{C}$, to, 180-345 $^{\circ}\text{C}$ and 345-580 $^{\circ}\text{C}$; and this when the particle size decreases respectively, from 0.5mm to 1.5mm [45].

4.2 Kinetic models

The mechanism of thermal decomposition of OMSW, could be described into three main models: single step (global reaction) model, multiple step model or semi global model [38]. The whole mechanism is decomposed on consecutive, parallel or both consecutive and parallel reactions as shown in (figure.4) and (figure.5).

4.2.1 Single step global reaction model

These models consider the thermal decomposition process as a global reaction, where the overall kinetic parameters could be determined from TG and DTG curves [38]. The single step model has been applied in OMSW torrefaction investigations and justify its adequacy with experimental kinetic data[18]. Indeed, The apparent activation energy (E_a) was around 200KJ.mol^{-1} along the conversion rates ($\alpha < 0.55$), in accordance with the weight loss (20-35%) of torrefied OMSW[18].

4.2.2 Multiple steps model

However, the single step models still usefulness to describe more complex mechanism occurring during OMSW thermal decomposition. Many authors investigated the thermal degradation of OMSW under multiple steps model assumptions, in order to predict kinetic behavior of OMSW and product yields[22]. The figure.4 gives an example of four-steps model used in kinetic investigation of OMSW slow pyrolysis[42].

The four steps kinetic model	
Reaction N°	Type
1	3-dim. diffusion janders type
2	n-th ordre
3	n-th ordre
4	n-th ordre
Model	
$A \xrightarrow{1} B \xrightarrow{2} C \xrightarrow{3} D \xrightarrow{4} E$	

Figure.4: Four-step model example from[42].

4.2.3 Semi-global model

This approach has attracted authors due to its ability to simplify the OMSW thermal decomposition into three simpler reactions, without further knowledge of the heterogeneous reactions occurring during the process [7, 38,48]. The figure.5 shows an example of simplified reactions scheme, which assume the OMSW pyrolysis occurring into three separate reactions viz, hemicellulose, cellulose and lignin decomposition[7]. Moreover, semi-global models are known for their capability to compare between different biomasses kinetic data, in term of their products. However, this approach remains non suitable to compare kinetic data from different operating conditions [38].

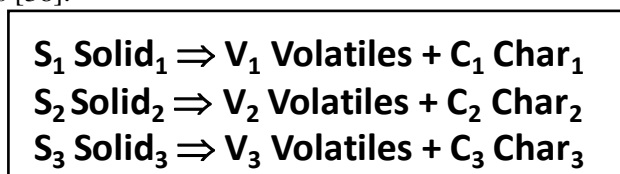


Figure.5:Example of proposed kinetic model for OMSW pyrolysis

4.4 Kinetic analysis techniques

Kinetic analysis techniques could be classified into three main classes, namely, iso-conversional methods, model based (model fitting) methods and non-linear regression methods [13].

4.4.1 Iso-conversional methods (Model free methods)

The prominence of iso-conversional methods has increased with the non-isothermal kinetics investigations [49]. The fundamental assumption of these methods considers that the reaction rate (da/dt) depends only on temperature (for a given conversion α) [13]. The most popular iso-conventional methods used in kinetic analysis are ASTM E698 (Kissenger), Fiedman, Flynn-Wall-Ozawa (FWO) and vyazovkin[13]. In these methods, the activation energy (E_a) is assumed as a conversion (α) function [13] and could be determined without the knowledge or specification of the reaction model $f(\alpha)$ [39].

4.4.2 Model-fitting methods (model based)

Contrary to iso-conversional methods, the model-fitting methods have been overwhelmingly used in isothermal kinetics investigations [49]. In these methods, the basic assumption is that the apparent energy is independent of temperature and stays constant throughout the decomposition temperature range [13]. The most common, model-fitting method used in thermal decomposition of biomass is the Coats-Redfern method [39, 42,44].

4.4.3 Non-linear regression analysis

The non-linear regression uses iterative procedures to almost fit a non-linear model to the experimental data [13]. In this line, the non-linear optimization method of Marquardt-Levenberg has been virtually used [47, 50]. In the other hand, the least square (LSQ) is also used to minimize the deviance term [47]. These techniques usually use software tools to perform the regression computation [50].

4.5 Thermal decomposition parameters

The OMSW thermal decomposition is a multifactorial process, which depends on several parameters. The aim of this section is to overview the effect of the common experimental conditions on the thermal decomposition behavior of OMSW.

4.5.1 Heating rate effect

In DTG curves basis, the heating rate has an important effect in the thermal degradation characteristics of OMSW. Indeed, an increase of devolatilization rate and the delay of complete char formation were observed, when heating rate increases [20]. Moreover, the ignition temperature, decreased from 237 °C to 183 °C when heating rate rise from 10 °C/min to 25 °C/min [20]. In contrast, the burnout temperature increased significantly from 534 °C to 839 °C for, respectively, 10 °C/min and 25 °C/min heating rates [20]. Finally, the combustion index raises with 2.4 times between 10 and 25 °C heating rates, ensuring better combustion intensity [20]. This behavior could be interpreted by the heat transfer limitation, which became more important when heating rates increased. Indeed, higher rating rates caused (lower combustion time) more important thermal shocks and greater gradient temperature along the OMSW thickness [39].

4.5.2 Particle size effect

The thermal decomposition mechanism depends widely on this parameter, and this is due to its contribution on heat and matter diffusion [39]. The lowest particle size ($d < 0.5$ mm) shows the highest rate conversion ($135 \mu\text{g s}^{-1}$) during volatilization stage, producing more volatiles (about 61%) and less of chars [45]. In turn, the ash yield decreases more than 5 times; from 6.2 % to 1.2 % when particle sizes increases from $d < 0.5$ mm up to 2 mm $< d < 2.8$ mm, respectively [45]. The effect of particle size in CO and CO₂ emissions during volatilization and char oxidation steps is also significant, where, the CO and CO₂ emissions increases conversely with the particle size during the volatilization step, in contrary, with char oxidation step where CO and CO₂ emissions increased when particle size increased [45]. Moreover, a delay in the ignition temperature of the both steps of OMSW decomposition was observed when the particle size raised [45, 46].

To avoid the erroneous of thermal analysis results during biomass thermal decomposition, the lowest particle size of samples are recommended [46].

4.5.3 Temperature effect

Naturally, the temperature is a fundamental parameter in thermal decomposition of OMSW, as it is well expressed by the Arrhenius equation. Furthermore, the thermolysis temperature has shown its effect on the thermolysis products yield [51]. In accordance with literature, the char yield from pyrolysis of OMSW decreases when temperature raises [15]. Moreover, a higher chars fixed carbon content, resulted from higher temperature pyrolysis [47]. In contrast, An increase in both the gas yield and its hydrogen content have been observed when pyrolysis temperature raises [15].

4.5.4 Pressure effect

The pressure effect has been investigated in the range 0.1-1.5 MPa and temperature range of 400-550 °C during two phase olive mill solid waste (TPOMSW) pyrolysis [47]. Therefore, a decrease in the char yield, produced along the TPOMSW pyrolysis, have been observed when the pressure increases along with [47]. In contrast, the fixed carbon yield increases with the TPOMSW pyrolysis pressure [47]. Finally, an optimal TPOMSW pyrolysis pressure (0.8 MPa) was determined in term of higher devolatilization rate [47].

4.5.5 Oxidation agent concentration effect

The devolatilization step of OMSW thermal degradation is not significantly affected by the oxidation agent (O₂). Nevertheless, the char oxidation step depends on the Oxygen concentration, which begins at lower temperatures when O₂ concentration increased [45]. In turn, the emissions from devolatilization are affected by the inlet Oxygen concentration, where CO and CO₂ concentration increased in the outlet gases with the increase of O₂ concentration in inlet carrier gas, due to the diffusion and adsorption of Oxygen by OMSW surface causing more CCF(O) decomposition [45]. Naturally, the rate conversion during the char oxidation step is a function of the inlet oxygen concentration. Moreover, ignition temperature of OMSW char oxidation varied from 346 °C to 320°C when the inlet oxygen concentration increased from 10 % to 20 % [45].

4.5.6 Catalysis agent effect

The dolomite effect, as a pyrolysis catalyst, has been investigated using a range of mass between 0 -100 g [15], on the tar, char and gaseous phases generated during the process for energy recovery usage. Tar and gas yields respond to the catalyst effect, and their standard deviation values are 3.17 and 3.38, respectively [15]. Indeed, the tar yield decreased as, 34.27%, 33.17%, 30.20% and 27.22% and the gas yield increased as, 41.73%, 43.24%, 46.21% and 49.39% for, respectively, 0, 16.8g, 49.7g, 100.04 g of dolomite mass at 700 °C [15]. In turn, the char yield was intact by the dolomite presence and mass raises of about 0.20 of standard deviation throughout the different assays [15]. However, the energy quality of the char has been enhanced along the different catalyst masses increasing as, 26.63, 29.72, 30.46, 30.50MJ/kg in despite of tar energy quality which decreased 3.60, 0.89, 0.45, 0.37 MJ/kg for, respectively, 0, 16.8g, 49.7g, 100.04g of dolomite mass at 700 °C [15]. Moreover, the H₂ fraction in gas increased (3.58, 10.79, 13.95 and 15.79%), as well as, the total HHV of gases (5.22, 6.44, 7.13 and 7.36MJ/Kg) for, respectively, 0, 16.8g, 49.7g, 100.04g of dolomite mass at 700 °C [15]. In contrast, the CO, CO₂ and CH₄ fractions decreased in the total gases when the dolomite mass increased [15]. The stability of dolomite, which was stable after six consecutive uses, was another positive criterion of dolomite use as catalyst [15].

5. Pre-treatment

5.1 Drying

The moisture content is an important factor that reduces the OMSW energy quality during the combustion process. Indeed, the contained water in raw material consumes its necessary evaporation energy from the raw material whole energy. Furthermore, many undesirable reactions occur due to the water presence in the olive raw material. In order to maximize the combustion energy efficiency and minimize the harmful consequent emissions, a drying pre-treatment of OMSW pre-treatment represents an appropriate solution.

Many previous investigations were investigated the forced convection drying of OMSW [41, 50, 52-56]. Some of these studies have investigated the influence of the experimental conditions on the drying characteristics, the drying time and, or the energy quality of the fuel product [41, 53, 54]. Others have been focused on the drying kinetics and, or adsorption/desorption isotherms of water content in OMSW [50, 56]. Furthermore, some authors are interested to the energy efficiency of OMSW drying process from a technological point of view at industrial scale [52, 55].

5.1.1 Drying kinetics

According to [41] the average moisture content for the OMSW drying could be expressed as follows:

$$M_R = \frac{(M - M_{eq})}{(M_0 - M_{eq})}$$

Where M_{eq} is the equilibrium moisture, M is the moisture content at a given time and M_0 is the initial moisture content. Until M_{eq} remains insignificant comparing to M and M_0 the average moisture content M_R could be simplified as follows:

$$M_R = \frac{M}{M_0}$$

on the other hand, the moisture content could be predicted by mathematical models, describing the moisture content profile as a time function [13]. Some simplest kinetic models, in particular, Page model and Henderson and Pabis model have been used to predict the OMSW drying behavior. These models express the moisture content as a time function. Then the models constant are fitted to the experimental data to determine an empirical equation describing drying curves of OMSW [41]:

$$\text{Page model: } M_R = \exp(-kt^y)$$

Henderson and Pabis model:
$$M_R = a \exp\left(-bt\right)$$

More complicated models have been assayed to describe the characteristic drying curve (CDC). An order 4 polynomial model has been proposed to describe the moisture loss during a convective solar drying of OMSW [50]. Otherwise, four drying kinetic models (namely, modified Halsey, modified Henderson, LESPAM and modified Oswin) have been compared to model the sorption isotherms of water by OMSW during drying process [56]. Finally, an exhaustive drying kinetic models list was presented by [13].

Moreover, the effective diffusivity could be determined from experimental data using Fick diffusion model. Then the activation energy might be fitted from Arrhenius equation, which expresses the effective diffusivity as temperature function [13].

5.1.2 Experimental conditions

The drying phenomena of OMSW consists of a combination of mass and heat transfer, and depends of both the sample proprieties and operating conditions [20].

5.1.2.1 Temperature

Many authors demonstrated the influence of temperature in drying behavior of OMSW. Indeed, a decrease in drying rate was observed when temperature increased for a given thickness. Consequently, high drying temperatures reduced the needed drying time, to reach the OMSW equilibrium moisture, and raises the effective diffusivity during the drying process [41, 50, 53, 54].

According to previous findings, the OMSW drying under three temperatures (60, 70 and 80 °C) has been investigated [53]. The associated velocity values at 60, 70 and 80 °C were $1.84 \cdot 10^{-7}$ m²/s, $3.03 \cdot 10^{-7}$ m²/s and $3.42 \cdot 10^{-7}$ m²/s, respectively [53]. The shortest drying time and the highest effective diffusivity corresponded to the highest temperature (80 °C) [41, 53].

5.1.2.2 Sample thickness effect

In contrast, the samples thickness influences conversely OMSW drying rate at constant temperature and velocity [41, 50, 53]. Indeed, The drying time decreases about 15.3% (from 260 min to 220 min), 9.1% (from 220 min to 200 min) and 16.6% (from 120 min to 100 min) at respectively, 40 °C, 60 °C and 80 °C when thickness sample passes from (1.5 cm to 0.5 cm) under 0.042 m³/s of air flow rate [50]. Furthermore, the effective diffusivity took higher values with thicker samples. Indeed, an important variation in effective diffusivity value, as follows: $34.1 \cdot 10^{-8}$ m²/s, $18.4 \cdot 10^{-8}$ m²/s and $7.22 \cdot 10^{-8}$ m²/s for respectively 1.5 cm, 1.0 cm and 0.5 cm of thickness at 80 °C and 0.083 m³/s of air flow rate [50].

However, a particular case [53] was observed, where the effective diffusivity decreased with sample thickness at 70 °C, while its value varied as 3.03 m²/s, 2.98 m²/s and 3.98 m²/s for respectively, 6 mm, 9 mm and 12 mm [53]. This behavior might be explained by the dependence of drying mechanism on samples thickness, because it changed from capillary mode, in thin layer (6 mm), to diffusion mode in thicker samples (9 and 12 mm), [53]. Finally, the activation energy is an increasing function of thickness, whose values were, 19.6, 24.2 and 30.3 KJ/mol for respectively, 0.5cm, 1.0cm and 1.5cm [50]. Other authors [53] were in accordance with this statement due, to the higher necessary energy to remove water from thicker samples [53]. Indeed, the obtained activation energy values were 25.4, 25.7 and 29.2 KJ/mol for respectively, 6 mm, 9 mm and 12 mm of thicknesses [53].

5.2 Torrefaction

Torrefaction is a mild pyrolysis process because of its low range temperature (200-300 °C) [57]. This process has been investigated as a prominent biomass pre-treatment way due to its following advantages [22]:

- ✓ Higher energy density.
- ✓ Higher hydrophobicity.
- ✓ Better reactivity during combustion, adsorption/desorption or catalysis use.
- ✓ Easier storage and transportation
- ✓ And better uniformity of biomass proprieties.

5.2.1 Torrefaction process and products

The biomass torrefaction is a thermo-chemical conversion process, where the raw biomass is heating in an inert atmosphere, at a range temperature of 200-300 °C and atmospheric pressure [18]. The torrefaction process could

be classified into slight, mild and severe torrefaction processes, according to the operating temperature (200-235 °C; 235-275 °C and 275-300 °C, respectively) [58].

The moisture content is the first eliminated fraction, which reacts at lower temperatures (around 105 °C). Then, hemicellulose represents the most thermo-reactive fraction of biomass that is decomposed at 220-315 °C. The hemicellulose could be mildly decomposed in slight and mild torrefaction as it could be severely decomposed in mild and severe torrefaction[22]. On the other hand, cellulose and lignin fractions could be slightly decomposed during slight and mild torrefaction. During severe torrefaction, a greater extent of cellulose could react, contrary to lignin which needs higher temperatures[22].

The hemicellulose and lignin decompositions are exothermic reactions while cellulose decomposition is an endothermic reaction in nature[22]. However, the cellulose decomposition could be driven in an exothermic sense by increasing the char yield, which competes with the tar formation[22]. This approach could be profitable from an energy efficiency point of view, where the whole torrefaction energy could be minimized. The torrefaction process generates three phases products (char, tar and volatiles) [57] Moreover, the torrefaction products yield of OMSW varied according, to its chemical composition as well as to its torrefaction conditions (torrefaction temperature and the retention time, etc)[58].

The main volatiles produced during torrefaction consist of carbon dioxide, carbon monoxide, possible traces of acetic acid, hydrogen, methane [57], toluene, benzene and C_xH_y [22]. Furthermore, the tar phase is mainly constituted from H_2O , acetic acids, alcohols, aldehydes and ketones [22]. Finally, the solid phase (char) is a carbon-enriched char, which contain more than 75% of initial energy content [57].

5.2.2 Proprieties of torrefied biomass (char):

The proximate composition of OMSW as well as its energy value and density undergo many changes during torrefaction process.

5.2.2.1 Moisture content

The moisture content is a crucial property in biomass fuels characterization, and that is for many reasons[22]:

- ✓ The energy value of the biomass fuel depends on the moisture content due to the necessary energy for the water evaporation along thermochemical conversion processes.
- ✓ The emissions along the thermochemical conversion process depend on the contained water and the other biomass constituents, why, a better dried biomass product ensure a better environment friendly operations.
- ✓ The moisture content accelerates the biological activity, and contributes to the product degradability and deterioration along the storage time.
- ✓ The storage and transportation costs could be minimized by moisture elimination.

A low OMSW moisture content has been reached (less than 1%) after several hours torrefaction in ambient atmosphere[59]. The torrefied OMSW has been qualified as a long term hydrophobic product[59].

5.2.2.2 Volatile matter (VM), fixed carbon (FC) and elemental contents

Volatile matter, fixed carbon and ash of OMSW undergo several changes under torrefaction conditions. Indeed, the VM content decreases throughout the torrefaction treatment while the (FC) and char yields increased [22]. Furthermore, an increase of FC and ash contents and a decrease of VM fraction were observed when the OMSW torrefaction temperature increased[21]. Indeed, the VM yield decreased as (77.65%, 72.63% and 61.71%), when temperature increased as (200 °C, 250 °C and 300 °C, respectively) for 45min of torrefaction retention time[21]. Moreover, the FC fraction increases as (16.79%, 22.23% and 30.62% at, respectively, 200 °C, 250 °C and 300 °C) for 45 min holding time. Finally, the ash content varied from 4.82% at 200 °C to 6.82% at 300 °C for 45 min of torrefaction holding time[21].

Aforesaid, the OMSW char moisture and VM contents, which are rich in oxygen and hydrogen, decreased during torrefaction process. Thus, the carbon content increases due to the fixed carbon fraction increase under torrefaction conditions[22].

Otherwise, the carbon content in OMSW char was more important when the torrefaction conditions were more severe[21]. Indeed, it progresses from 51.70% at 200 °C to 66.39% at 300 °C for 45min of torrefaction retention time[21]. In contrast, the oxygen content decreased from 35.95% at 200 °C to 19.94% at 300 °C for 45min of torrefaction retention time[21]. In turn, the Hydrogen showed less important variations under torrefaction conditions, varying from 6.18% at 200 °C to 5.55% at 300 °C. Finally, the nitrogen and Sulphur contents remain nearly constant during torrefaction process[21]. In fact, the atomic O/C and H/C ratios of OMSW decrease during torrefaction process. Furthermore, the decrease of O/C and H/C induces an increase

in hydrophobicity and GCV value of OMSW [58]. Hence, the torrefaction process could be qualified as a suitable pretreatment for the enhancement of OMSW energy value[58].

5.2.2.3 Solid yield, energy density and energy yield

The solid yield (SY) is defined as the ratio of the final mass and the initial one. It represents the non-lost mass during torrefaction[22]. Other investigations have opted for another parameter which is the anhydrous weight loss (AWL). This parameter represents the lost fraction after torrefaction [59].

$$SY = \frac{m_f}{m_0}[22]$$

$$AWL = 1 - \frac{m_f}{m_0}[59]$$

Where: m_f and m_0 are the torrefied and initial masses of OMSW.

In this sense, defined The enhancement factor is defined as the GCVs ratio of torrefied and raw OMSWs, [22]:

$$EF = \frac{GCV_f}{GCV_0}[22]$$

Where: GCV_f and GCV_0 are the torrefied and raw OMSW gross calorific values.

The main goal of torrefaction is the enhancement of the GCV values of biomass fuels. Hence, the enhancement factor is always greater than unity[22].

Finally, the energy yield or calorific yield (CY) is defined as the energy available ratio of torrefied and raw matters[22]:

$$CY = \frac{m_0 \cdot HHV_f}{m_f \cdot HHV_0}$$

Or

$$CY = SY \cdot EF[22]$$

$$CY = (1 - AWL) \cdot EF [59]$$

The energy (CY) is the measure that interprets the contribution of the process to the torrefied fuel. Otherwise, it is the efficiency of the torrefaction process to enhance the energy form of OMSW stored in chemical form [58].

Finally, It has been proved that torrefaction under severe conditions has been efficient to enhance the torrefied OMSW energy value [58]. However, a longer torrefaction retention time (>30min) lead to a loss in the torrefied OMSW chemical energy (up to 40%) [58].

6. Energy uses of OMSW

6.1 Pyrolysis

Previous researches ascertain that OMSW pyrolysis could be classified into slow [42], fast [51] and flash pyrolysis. The three classes could be distinguished by the operating conditions such as heating rate, temperature, holding time, and particle size. Therefore, the pyrolysis products are the char, tar and gas [13].

The pyrolysis process is an important thermochemical conversion phenomenon which is largely used in different biomass industrial and experimental fields, due to its economic and ecological benefits [38]. Moreover, the pyrolysis process application could be driven, by controlling the operating parameters, in term of the product yields (tar, char, gas), as well as, their compositions (as described in “3.4. Thermal decomposition parameters”section). Indeed, the industrial pyrolysis applications cover a large scale of applications as a unit operation (torrefaction, combustion, gasification, carbonization, etc). Furthermore, the pyrolysis process is hugely used in the synthesis and the refining of bio-oil and gases, notably, in olefins industry, in aromatics industry, in H_2 catalytic synthesis, in catalytic cracking or in methanol transformation to olefins [46].

On the other hand, the pyrolysis process has been performed in a large scale of reactors, namely, fluidized bed reactors [60, 61], transport and circulating fluidized bed reactors [8], bubbling fluidized bed reactors [62], ablative reactors, auger reactors, vacuum reactors and conical spouted bed reactors [46]. However, the pyrolysis process is a high consuming energy technology, due to the high required temperatures. In fact, many researchers have discussed the pyrolysis energy efficiency pathways, by driving the products yields and reducing the endothermicity of the process [22]. In this case by addition of low oxygen concentration involving more exothermic reactions [46] and/ or by-products use to reach auto-thermal regime [45]. Several investigations have addressed the OMSW pyrolysis in the last decade [7, 14, 15, 17, 21, 40, 42, 47, 51]. Many authors have studied the pyrolysis behavior of OMSW and analyzed the effect of operating conditions such as temperature [51], pressure[47], catalyst agent (dolomite) [15], on products composition[17] and their energy quality [21]. Furthermore, their kinetic analysis was approached by several investigations [7, 14, 40, 42,47].

6.2 Combustion/co-combustion

The combustion process refers to the fuels burning, in excess air, producing heat energy [13]. As described, in the thermochemical decomposition section, the combustion mechanism could be described as two successive mechanisms where the pyrolysis process occurs in the first step followed by the char oxidation step.

Many authors have been interested to The OMSW combustion, and this to assess the energy potential of biomass as solid fuel [9, 14, 17, 19, 40, 44, 45, 48, 59, 63], influence of combustion parameters[63], combustion kinetics [14, 48, 59], combustion emissions [64], and combustion modelling[19].

The co-combustion term is used when two, or more, fuels are combined with the main fuel and burned simultaneously in the same chamber of combustion [13]. This technique is used for its large benefits in reducing the greenhouse gases emissions (CO_2 , CH_4 , etc), as well as, other pollutants (NO_x , SO_2 , etc) per unit of produced energy [40]. The co-combustion of OMSW with coal was investigated by several authors, in order to, (i) assess the combustion performances and emissions rate [62]; (ii) determine the optimum operating parameters, in terms of, energy efficiency and combustion emissions [65]; (iii) and enhance the furnace design, in order to reduce the polluting emissions rate [61]. In the other hand, the co-combustion behavior of two phase olive mill solid waste (2-PH), three phase olive mill solid waste (3-PH) and olive tree pruning (PR) was studied [20] in different ratios. Finally, the lowest activation energy corresponded to the mix of 25% (PR) and 75% (2-PH), while the raw (PR) represented the highest one [20].

6.3 Gasification

The gasification process has received a growing interest of researchers, as alternative to combustion. Indeed, the syngas combustion represents higher performances compared to solid fuels, in term of thermodynamic efficiency. Moreover, the gasification is a cleaner process than combustion, due to its lower pollutants emissions[5]. In the other side, OMSW has shown a high reactivity during gasification in comparison to other biomasses. Indeed, its high ash content in minerals, especially the potassium oxides, catalyzes the gasification process [40].

Several investigations have focused on the thermo-economic assessment of OMSW gasification process [66-68]. Indeed, a life cycle olive wastes management strategy was proposed for a 10hectars scale farm[66]. Gasification and pyrolysis were assessed as energy recovery techniques for both electrical and thermal energy production [66]. Otherwise, the remaining char might be used for the farm soil amendment[66]. Both scenarios (gasification or pyrolysis), could cover the local farm energy consumption, and ensure a surplus energy production [66]. In the other hand, a thermo-economic assessment of a combined heating and power (CHP) generation plant (800 KWt and 200 KWe of thermal and electrical powers generation, respectively), has been investigated [67]. Despite, the low net calorific value of synthesized gas ($4.8\text{-}5.0\text{MJ}\cdot\text{Nm}^{-3}$), the plant investment has been qualified as cost efficient [68].

7. Activated carbon

The OMSW and olive stones have been thoroughly studied as low cost adsorbent precursors, these last decades. Their surface proprieties attracted many researchers in depollution fiel. Indeed, the large surface area (up to $1839\text{m}^2/\text{g}$), the high porosity up to $0.86\text{ m}^3/\text{g}$ as well as abundant functional groups [13] make these biomass as high potential precursor for activated carbon preparation.

7.1 Activation process

The OMSW activation refers to different chemical and physical processes, which aim to enhance the surface and porosity proprieties of OMSW as well as its adsorption proprieties for further adsorption or catalytic applications[69]. According to literature, OMSW and olive stones activation has been preceded using different treatments, viz., carbonization, chemical activation and hydrothermal treatment. The table.1 resumes the different processes used in OMSW and olive stones activation, and surface proprieties of activated samples.

7.1.1. Pyrolysis

The pyrolysis, or carbonization, allowed an important enhancement in term of surface area and porosity of carbonized OMSW and olive stones. Pyrolysis temperature varied between 400 and 850 °C, it had an important effect in both carbon weight loss and activated carbon properties [31, 70]. Indeed, the carbonization of olivestone at 800°C for 60min allowed reaching $500\text{m}^2/\text{g}$ of surface area[30]. However, higher pyrolysis temperatures involved macro-pores development and a decrease in total surface area [29].

7.1.2. Chemical activation

The chemical activation of OMSW has been largely studied in literature using several dehydrating agents (KOH, NaOH, ZnCl₂, H₃PO₄, HNO₃, H₂SO₄). Many authors investigated the OMSW activation using a simple dehydrating agent as (H₃PO₄, H₂SO₄, HNO₃, NaOH), while others opted for a second chemical modification (i.e H₃PO₄ activation followed by HNO₃ or KMnO₄ treatments). The combination of carbonization and chemical activation allowed a well development on OMSW and olive stones surface proprieties. Indeed, the activation of carbonized OMSW at 450 and 800 °C using ZnCl₂ and KOH, respectively, allowed to reach 1480m²/g and 1839m²/g, respectively. Moreover, the micro-pores represented more than 80% of total pores volume, which reached 0.859cm³/g.

7.1.3. Physical activation

On the other hand, the physical activation by CO₂, or water steam have been used to enhance the material porosity and surface area. [16, 34]. The physical activation (CO₂ and steam activations) methods allowed to reach high values of surface area (1030m²/g and 1591 m²/g, respectively), as well as total volume pores (0.75cm³/g and 1.56 cm³/g, respectively). Nevertheless, the steam activation methods showed more tendency to meso then macro-pores, according to the pyrolysis temperature, as shown in table.1.

7.2 Potential application of OMSW adsorbents

The OS and OMSW precursors have attracted many researchers in depollution field for their capacity to uptake several gaseous and liquid pollutant effluents, especially, heavy metals, dyes, organic matter and gases [16, 31, 34, 63, 71]. The preparation conditions, as well as adsorption parameters (pH and temperature) determine the adsorbent capacity toward contaminants. The table 3 shows the capacity of treated OMSW and olive stones (OS) towards various pollutant particles.

Table 2 : Potential application in depollution field of olive oil solid waste and olives stones.

Table 2a: Gases

Substrate	Capacity (mg/g)	AC	Treatments	pH	T (°C)	References
NO ₂	131	OS	water vapor activation (750°C)	-	20	[34]
CO ₂	418.88	OS	Carbonized olive stones	-	Room T.	[82]
Nitrite Ion	0.23	OS	Carbonized at 450°C for 2h	4	25	[31]
Nitrite Ion	0.45	OS	Carbonized at 450°C for 2h then activated by H ₃ PO ₄	4	25	[31]
Nitrite Ion	2.25	OS	Carbonized at 450°C for 2h then activated by ZnCl ₂	4	25	[31]

Table 2d: Phenols [83]

Substrate	Capacity (mg/g)	AC	Treatments	pH	T (°C)	References
Caffeic acid	284.59	OMSW	carbonized at 800°C for 1h then activated using KOH at 800°C for 3h	3.2-3.5	25	[27]
Vanillin	191.41	OMSW	carbonized at 800°C for 1h then activated using KOH at 800°C for 3h	3.2-3.5	25	[27]
Vanillic acid	148.23	OMSW	carbonized at 800°C for 1h then activated using KOH at 800°C for 3h	3.2-3.5	25	[27]
p-Hydroxybenzoic acid	101.01	OMSW	carbonized at 800°C for 1h then activated using KOH at 800°C for 3h	3.2-3.5	25	[27]
Gallic acid	83.84	OMSW	carbonized at 800°C for 1h then activated using KOH at 800°C for 3h	3.2-3.5	25	[27]

Table 2b: Heavy metals

Substrate	Capacity (mg/g)	AC	Treatments	pH	T (°C)	References
Cd(II)	65.4	OS	Washed(distillated water) and dried	6	28	[72]
Cd(II)	20	OMSW	Pyrolised and activated by ZnCl ₂	-	25	[73]
Cd(II)	200	OS	esterified with succinic anhydride in toluene	4	18-22	[74]
Cd(II)	128.2	OS	Activated by H ₂ SO ₄ at room temp followed by NaOH neutralization	4	-	[75]
Cu(II)	35.3	OMSW	Activated by H ₃ PO ₄ followed by carbonization	4.79	23-25	[71]
Cu(II)	31.75	OMSW	Activated by H ₃ PO ₄	5	Room T.	[76]
Pb(II)	14.109	OS	Activated by H ₂ SO ₄	5	-	[26]
Pb(II)	15.345	OS	Activated by HNO ₃	5	-	[26]
Pb(II)	16.247	OS	Activated by NaOH	5	-	[26]
Pb(II)	6.39	OMSW	Dried and milled(<1mm)	5	25	[77]
Pb(II)	23.7	OS	Dried and milled(<1mm)	5	25	[77]
As(III)	1.39	OS	Activated using K ₂ CO ₃ and carbonized	-	-	[28]
Zn(II)	6.7	OMSW	(>2mm)	6.5	25	[78]
Zn(II)	33.56	OMSW	Carbonized at 850°C for 2h	>8	25	[29]
Fe(III)	0.485	OS	Washed(cold then hot water) and dried	2.9	70	[16]
Cr(VI)	12.15	OMSW	Washed(distillated water) dried and milled (<1mm)	2	25	[25]
Cr(III)	4.99	OS	milled (<1mm)	4	25	[79]
Hg(II)	104.59	OMSW	Carbonized at 630°C	-	25	[80]
Boron	1.05	OS	Acid phosphoric activation followed by 500°C carbonization	9.26	25	[33]
Boron	3.5	OMSW	Carbonized at 500°C then activated by steam at 850°C for 45min	5.5	25	[37]

Table 2c: Dyes

Substrate	Capacity (mg/g)	AC	Treatments	pH	T (°C)	References
BM	3.296	OS	milled (<1mm)	7.0-8.0	25	[79]
Basic green 4	41.66	OMSW	Dried and milled	4.5	25	[81]
Safranine	526.3	OS	Acid sulphuric at room temp followed by NaOH neutralization	6.8	-	[75]

Conclusions

The olive mill solid wastes have been largely studied for different purposes. Indeed, the increase of interest in the olive oil industry and the huge generated quantities require the development of adequate and alternative management solutions. The present document highlights the most prominent valorization pathways of OMSW, namely, energy recovery and activated carbon preparation. The gross calorific value of OMSW makes far potential and renewable resource of energy. Drying and torrefaction are the most used treatment to prepare a solid biofuel from, while gasification and pyrolysis represents a prominent option which attracts many researchers, as alternatives to OMSW combustion.

The surface proprieties of OMSW and olive stones show more prominent options for OMSW valorization. The activated carbon prepared from OMSW and olive stones attracted the science community for its high depollution capacity toward different pollutant particles, in particular, heavy metals, dyes, organic matter and gases. Otherwise, the valorization of OMSW has been largely studied and different thermochemical and biotechnological processes have been assessed as alternative valorization pathways. Indeed, the bio digestion of OMSW was subject of several investigations in renewable energy field. Moreover, OMSW composting has been investigated and showed many advantages as valorization pathway. Finally, let's mention that other applications and valorization pathways have been investigated in the last decades, namely, masonry bricks and other materials preparation, compounds extraction and medicinal applications.

Acknowledgment:

This work was financially supported by the VGOLIVES Project; the Ministry of Energy, Mining, Water and Environment, Morocco.

References

1. Council ioo. Olive oils production market newsletter, n° 110 – November 2016.
<http://www.internationaloliveoil.org/documents/viewfile/11716-market-newsletter-november-2016>.
2. Albuquerque J.A., González J., García D., Cegarra J., *Bioresource Technology* 91 (2004) 195-200.
3. Akay F., Kazan A., Celiktas M.S., Yesil-Celiktas O., *The Journal of Supercritical Fluids* 99 (2015) 1-7.
4. Bhada-Tata P.H., Daniel A., What a waste? : a global review of solid waste management. The world bank,
<http://documents.banquemonde.org/curated/fr/302341468126264791/What-a-waste-a-global-review-of-solid-waste-management> (2014).
5. Kalderis Dimitrios DE., *Terrestrial and Aquatic Environmental Toxicology* 4 (2010) 7-20.
6. Dalmasso AAEC., Unité de valorisation complète de déchets oléicoles par lombricompostage : Production de produits à haute valeur ajoutée : lombricompost, savon, collagène et lombrics (2012-2013).
7. García GB., Calero de Hoces M., Martínez García C., Cotes Palomino MT., Gálvez AR., Martín-Lara MÁ., *Fuel Processing Technology* 126 (2014) 104-111.
8. García-Ibañez P., Cabanillas A., Sánchez JM., *Biomass and Bioenergy* 27 (2004) 183-194.
9. Miranda T., Esteban A., Rojas S., Montero I., Ruiz A., *International Journal of Molecular Sciences* 9 (2008) 512.
10. Oreopoulou V., Russ W. *Utilization of by-products and treatment of waste in the food industry*. Springer, New York. (2007).
11. Dermeche S., Nadour M., Larroche C., Moulti-Mati F., Michaud P., *Process Biochemistry* 48 (2013) 1532-1552.
12. Vassilev SV., Baxter D., Andersen LK., Vassileva CG., *Fuel* 89 (2010) 913-933.
13. Christoforou E., Fokaides PA., *Waste Management* 49 (2016) 346-363.
14. Jauhiainen J., Conesa JA., Font R., Martín-Gullón I., *Journal of Analytical and Applied Pyrolysis* 72 (2004) 9-15.
15. Encinar JM., González JF., Martínez G., González JM., *Fuel Processing Technology* 89 (2008) 1448-1455.
16. Hodaifa G., Ochando-Pulido JM., Driss Alami SB., Rodriguez-Vives S., Martinez-Ferez A., *Industrial Crops and Products* 49 (2013) 526-534.
17. Mehmetli E., Dogan Ö., Tiris M., Kiran NC., Matuschek G., *CLEAN – Soil, Air, Water* 36 (2008) 315-319.
18. Brachi P., Miccio F., Miccio M., Ruoppolo G., *Fuel Processing Technology* 130 (2015) 147-154.
19. Zhong W., Xie J., Shao Y., Liu X., Jin B., *Applied Thermal Engineering* 88 (2015) 322-333.
20. Buratti C., Mousavi S., Barbanera M., Lascaro E., Cotana F., Bufacchi M., *Bioresource Technology* 214 (2016) 266-275.

21. Volpe R., Messineo A., Millan M., Volpe M., Kandiyoti R., *Energy* 82 (2015) 119-127.
22. Chen W-H., Peng J., Bi XT., *Renewable and Sustainable Energy Reviews* 44 (2015) 847-866.
23. Barbanera M., Lascaro E., Stanzione V., Esposito A., Altieri R., Bufacchi M., *Renewable Energy* 88 (2016) 185-191.
24. De La Casa JA., Castro E., *Construction and Building Materials* 61 (2014) 320-326.
25. Malkoc E., Nuhoglu Y., Dundar M., *Journal of Hazardous Materials* 138 (2006) 142-151.
26. Blázquez G., Calero M., Ronda A., Tenorio G., Martín-Lara MA., *Journal of Industrial and Engineering Chemistry* 20 (2014) 2754-2760.
27. Michailof C., Stavropoulos GG., Panayiotou C., *Bioresource Technology* 99 (2008) 6400-6408.
28. Budinova T., Petrov N., Razvigorova M., Parra J., Galiatsatou P., *Industrial & Engineering Chemistry Research* 45 (2006) 1896-1901.
29. Galiatsatou P., Metaxas M., Kasselouri-Rigopoulou V., *Journal of Hazardous Materials* 91 (2002) 187-203.
30. Spahis N., Addoun A., Mahmoudi H., Ghaffour N., *Desalination* 222 (2008) 519-527.
31. Zyoud A., Nassar HNI., El-Hamouz A., Hilal HS., *Journal of Environmental Management* 152 (2015) 27-35.
32. Abdel-Ghani NT., El-Chaghaby GA., ElGammal MH., Rawash E-SA., *New Carbon Materials* 31 (2016) 492-500.
33. Jaouadi M., Hbaieb S., Guedidi H., Reinert L., Amdouni N., Duclaux L., *Journal of Saudi Chemical Society* 2016 *in press*.
34. Ghouma I., Jeguirim M., Dorge S., Limousy L., Matei Ghimbeu C., Ouederni A., *Comptes Rendus Chimie* 18 (2015) 63-74.
35. González JF., Román S., Encinar JM., Martínez G., *Journal of Analytical and Applied Pyrolysis* 85 (2009) 134-141.
36. Wahby A., Abdelouahab-Reddam Z., El Mail R., Stitou M., Silvestre-Albero J., Sepúlveda-Escribano A., Rodríguez-Reinoso F., *Adsorption* 17 (2011) 603-609.
37. Köse TE., Demiral H., Öztürk N., *Desalination and Water Treatment* 29 (2011) 110-118.
38. White JE., Catallo WJ., Legendre BL., *Journal of Analytical and Applied Pyrolysis* 91 (2011) 1-33.
39. Garcia-Maraver A., Perez-Jimenez JA., Serrano-Bernardo F., Zamorano M., *Renewable Energy* 83 (2015) 897-904.
40. Senneca O., *Fuel Processing Technology* 88 (2007) 87-97.
41. Doymaz I., Gorel O., Akgun NA., *Biosystems Engineering* 88 (2004) 213-219.
42. Özveren U., Özdoğan ZS., *Biomass and Bioenergy* 58 (2013) 168-179.
43. Guida MY., Bouaïk H., Tabal A., Hannioui A., Solhy A., Barakat A., Aboulkas A., El harfi K., *Journal of Thermal Analysis and Calorimetry* 123 (2016) 1657-1666.
44. Álvarez A., Pizarro C., García R., Bueno JL., Lavín AG., *Bioresource Technology* 216 (2016) 36-43.
45. Chouchene A., Jeguirim M., Khiari B., Zagrouba F., Trouvé G., *Resources, Conservation and Recycling* 54 (2010) 271-277.
46. Amutio M., Lopez G., Aguado R., Artetxe M., Bilbao J., Olazar M., *Fuel* 95 (2012) 305-311.
47. Manyà JJ., Roca FX., Perales JF., *Journal of Analytical and Applied Pyrolysis* 103 (2013) 86-95.
48. Font R., Rey MD., Garrido MA., *Journal of Analytical and Applied Pyrolysis* 108 (2014) 68-77.
49. Vyazovkin S., *Isoconversional Kinetics of Thermally Stimulated Processes*. Springer International Publishing, Cham, (2015) 27-62.
50. Koukouch A., Idlimam A., Asbik M., Sarh B., Izrar B., Bostyn S., Bah A., Ansari O., Zegaoui O., Amine A., *Renewable Energy* 101 (2017) 565-574.
51. Uzun BB., Pütün AE., Pütün E., *Journal of Analytical and Applied Pyrolysis* 79 (2007) 147-153.
52. Torrecilla JS., Aragón JM., Palancar MC., *European Journal of Lipid Science and Technology* 108 (2006) 913-924.
53. Göğüş F., Maskan M., *Journal of Food Engineering* 72 (2006) 378-382.
54. Montero I., Miranda T., Arranz JI., Rojas CV., *International Journal of Molecular Sciences* 12 (2011) 7885-7897.
55. Messineo A., Volpe R., Asdrubali F., *Energies* 5 (2012) 1384.
56. Koukouch A., Idlimam A., Asbik M., Sarh B., Izrar B., Bah A., Ansari O., *Energy Conversion and Management* 99 (2015) 221-230.
57. Benavente V., Fullana A. T., *Biomass and Bioenergy* 73 (2015) 186-194.
58. Cellatoğlu N., İlkan M., *Torrefaction of Solid Olive Mill Residue* 10 (2015) 5876-5889

59. Guizani C., Haddad K., Jeguirim M., Colin B., Limousy L., *Energy* 107 (2016) 453-463.
60. Brachi P., Chirone R., Miccio F., Miccio M., Picarelli A., Ruoppolo G., *Fuel* 128 (2014) 88-98.
61. Akpulat O., Varol M., Atimtay AT., *Bioresource Technology* 101 (2010) 6177-6184.
62. Atimtay AT, Varol M., *Fuel* 88 (2009) 1000-1008.
63. Bouknana D., Hammouti B., Salghi R., Jodeh S., Zarrouk A., Warad I., Aouniti A., Sbaa M., Physicochemical Characterization of Olive Oil Mill Wastewaters in the eastern region of Morocco, *J. Mater. Environ. Sci.* 5 (4) (2014) 1039-1058
64. Jauhiainen J., Martin-Gullon I., Conesa JA., Font R., *Journal of Analytical and Applied Pyrolysis* 74 (2005) 512-517.
65. Cliffe KR., Patumsawad S., *Waste Management* 21 (2001) 49-53.
66. Zabaniotou A., Rovas D., Monteleone M., *Waste and Biomass Valorization* 6 (2015) 831-842.
67. Borello D., De Caprariis B., De Filippis P., Di Carlo A., Marchegiani A., Pantaleo AM., Shah N., Venturini P., *Energy Procedia* 75 (2015) 252-258.
68. Vera D., Jurado F., Panopoulos KD., Grammelis P., *International Journal of Energy Research* 36 (2012) 355-367.
69. Kambo HS., Dutta A., *Renewable and Sustainable Energy Reviews* 45 (2015) 359-378.
70. Cimino G., Cappello RM., Caristi C., Toscano G., *Chemosphere* 61 (2005) 947-955.
71. Baccar R., Bouzid J., Feki M., Montiel A., *Journal of Hazardous Materials* 162 (2009) 1522-1529.
72. Al-Anber ZA., Matouq MAD., *Journal of Hazardous Materials* 151 (2008) 194-201.
73. Aljundi IH., Jarrah N., *Journal of Analytical and Applied Pyrolysis* 81 (2008) 33-36.
74. Aziz A., Elandaloussi EH., Belhalfaoui B., Ouali MS., De Ménorval LC., *Colloids and Surfaces B: Biointerfaces* 73(2009) 192-198.
75. Aziz A., Ouali MS., Elandaloussi EH., De Menorval LC., Lindheimer M., *Journal of Hazardous Materials* 163 (2009) 441-447.
76. Martín-Lara MA., Pagnanelli F., Mainelli S., Calero M., Toro L., *Journal of Hazardous Materials* 156 (2008.) 448-457.
77. Blázquez G., Calero M, Hernáinz F., Tenorio G., Martín-Lara MA., *Chemical Engineering Journal* 160 (2010) 615-622.
78. Fernando A., Monteiro S., Pinto F., Mendes B., *Sustainability* 1 (2009) 277.
79. Trujillo MC., Martín-Lara MA., Albadarin AB., Mangwandi C., Calero M., *Desalination and Water Treatment* 57 (2016) 17400-17410.
80. Hanandeh AE., Abu-Zurayk RA., Hamadneh I., Al-Dujaili AH., *Water Science and Technology* 74 (2016) 1899-1910.
81. Koçer O., Acemioğlu B., *Desalination and Water Treatment* 57 (2016) 16653-16669.
82. Djeridi W., Ouederni A., Mir LE., *International Journal of Environmental Engineering* 8 (2016) 110-123.
83. Jodeh S., Hamed O., Mohamed M., Ben Hadda T., Hammouti B., Salghi R., Radi S., A. Abu Obaid, I. Warad, Removal of Phenol from Olive Industry Liquid Waste Using Polyitaconic Acid, *Asian J. Chem.*, 26 N°S(2014)S15-S22

(2017) ; <http://www.jmaterenvironsci.com>